Vol. 647: 149–160, 2020
https://doi.org/10.3354/meps13414

MARINE ECOLOGY PROGRESS SERIES
Mar Ecol Prog Ser

Published August 13

Stable isotopes of amino acids from reef fishes uncover Suess and nitrogen enrichment effects on local ecosystems

A. J. M. Sabadel[1,*], L. M. Durante[2], S. R. Wing[2]

[1]Department of Zoology, University of Otago, PO Box 56, Dunedin 9054, New Zealand
[2]Department of Marine Science, University of Otago, PO Box 56, Dunedin 9054, New Zealand

ABSTRACT: In 1979, the Suess effect was described as decreasing $\delta^{13}C$ in the oceans linked to anthropogenic CO_2 emissions. After years of over-fertilization of farming soils and runoff, we hypothesized that $\delta^{15}N$ in coastal environments would also decline, whereby synthetic fertilizers lead to depletion of the heavy isotope ^{15}N. We used museum-preserved and modern samples of 3 fishes from Otago, New Zealand, to reconstruct the isotopic baselines of C and N and assess specific trophic positions through time (1955–present) based on bulk and amino acid stable isotope values. Our sample set included *Odax pullus*, a strictly herbivorous species, and 2 commercially important species: *Nemadactylus macropterus* and *Parapercis colias*. Muscle tissue of the fishes recorded the change in $\delta^{13}C_{Bulk}$ through time, which matched estimated Suess effect values for New Zealand. We also resolved the effects on the C isotopic baseline from natural changes in the food web using analysis of the $\delta^{13}C$ of essential amino acids and found that while *P. colias* maintained a steady diet, the food web position of *N. macropterus* likely changed. Analysis of $\delta^{15}N$ of phenylalanine in *O. pullus* indicated a decrease of 0.023‰ yr^{-1} since 1955, which corroborates our coastal N-enrichment hypothesis. Furthermore, we found that isotopic changes for *N. macropterus* were consistent with overfishing and habitat degradation in the region. These data provide vital information for our resolution and understanding of how past environments have changed in terms of both anthropogenic influences on coastal food web structure and biogeochemical cycles of C and N in marine ecosystems.

KEY WORDS: Food web · Isotope baseline · Amino acid · Suess effect · Nitrogen enrichment · Coastal ecosystem

1. INTRODUCTION

The impacts of anthropogenic activities have become increasingly evident in both coastal and open ocean environments, with consequences for the structure and function of marine ecosystems (Harley et al. 2006, Shackell et al. 2010). By reconstructing and characterizing food webs through time, it is possible to better understand the modifications forced upon our modern ecosystems and predict their reactions to ongoing anthropogenic activities, as well as the legacy effects of past changes to biogeochemical cycles.

Stable isotopes have proven to be an effective tool to shed light on food web position and/or movement of a given population (Fry 2006). While bulk stable isotopes have their advantages and limitations, compound-specific stable isotope analysis of amino acids (CSIA-AA) can provide a valuable complementary approach to fine-tune our understanding of an ecosystem and its history. As the building blocks of proteins, amino acids (AAs) play a fundamental role in

*Corresponding author: amandine.sabadel@otago.ac.nz

Publisher: Inter-Research · www.int-res.com

all metabolic processes (O'Connell 2017) and their stable isotopes of carbon and nitrogen ($\delta^{13}C_{AA}$ and $\delta^{15}N_{AA}$, respectively) represent a powerful tool that has been widely applied to disentangle past (Pomerleau et al. 2017, Zupcic-Moore et al. 2017, Vokhshoori et al. 2019) and present (McMahon et al. 2016, Sabadel et al. 2016, Hetherington et al. 2017) food web structure. Indeed, some $\delta^{15}N_{AA}$ values (e.g. glutamic acid, $\delta^{15}N_{Glx}$) fractionate substantially between trophic levels while others (e.g. phenylalanine, $\delta^{15}N_{Phe}$) undergo very little fractionation (Popp et al. 2007), enabling precise calculation of the trophic position (TP) of an organism (Chikaraishi et al. 2009). Moreover, $\delta^{15}N_{Phe}$, as well as the $\delta^{13}C$ of essential AAs ($\delta^{13}C_{EAA}$) of primary producers can record environmental variations, such as changes in temperature, CO_2, and/or nutrient concentration (Yamaguchi & McCarthy 2018, Sabadel et al. 2019), thus representing a solid baseline to track changes in the isotopic composition at the base of a food web through time. This ability is particularly valuable in situations where isotopic information on the position of the base of the food web is lacking, such as in archaeological and paleontological studies. Recent studies have indicated that it is possible to use fixed/preserved museum specimens to reconstruct past trends in food web structure (Hannides et al. 2009, Hetherington et al. 2019). Indeed, $\delta^{13}C_{AA}$ used to track organic matter sources are not affected by fixatives or time under fixation (Chua et al. 2020, Durante et al. 2020b). Conversely, while $\delta^{15}N_{AA}$ values tend to vary between treatments, the authors found that for most fish, this variation is largely within the precision of the measurements and related to time between specimen collection and fixation. Moreover, the homogeneity of change of all individual AA values still allows for precise measurements of TP for historic samples (Durante et al. 2020b).

Since the industrial revolution, the decreasing amount of atmospheric $^{13}CO_2$ has changed the overall ratio of $^{13}C/^{12}C$ in natural systems. This phenomenon, termed the '^{13}C Suess effect' (Keeling 1979) also affects the isotopic ratio of the C diffused into the oceans and can vary from region to region (Gruber et al. 1999). The Suess effect has not yet been fully studied as it is resolved by $\delta^{13}C_{AA}$, but the few studies that have mentioned it, such as those in deep-sea coral tissues or historic samples from whales, found that the $\delta^{13}C_{EAA}$ values precisely recorded changes in inorganic C flux and changes in $\delta^{13}C$ values (Ruiz-Cooley et al. 2014, Schiff et al. 2014, McMahon et al. 2015a, Zupcic-Moore et al. 2017). Additionally, marine coastal ecosystems have also seen an increasing and continuous amount of artificial N added to their environment via the use of synthetic fertilizers applied to intensified farming, along with other animal manure, human sewage, and industrial sources. These anthropogenic inputs of NO_x into the environment have been shown to affect the $\delta^{15}N_{Bulk}$ baseline, as recorded in ice cores (Felix & Elliott 2013), lake sediments (Hundey et al. 2016), and coastal marine environments (Marion et al. 2005, Baker et al. 2010); but to our knowledge, the impact of artificial N on $\delta^{15}N_{AA}$ values in marine environments has, to date, not been investigated.

Therefore, the goal of the present study was to apply bulk isotopic analysis and CSIA-AA to investigate how C and N isotopic baselines have changed over time in a coastal region (Otago, New Zealand) due to anthropogenic activities, using fish muscle tissue samples. Indeed, between 1990 and 2001, New Zealand expanded the use of inorganic fertilizers for agriculture, with an increase of more than 450% on the land-based input of N through fertilizer application in the Otago region, reaching 530% by 2010 (Parfitt et al. 2012). In addition, the offshore subtropical waters on the shelf of the Otago region, which are typically depleted in N-containing nutrients (Van Hale & Frew 2010), have seen the N loading of estuarine and coastal environments increase markedly in recent years (Thrush et al. 2013). In this context, anthropogenic N depleted in the heavy isotope ^{15}N is added into the soils and leaches to the oceans, which is then used by primary producers and enters the local food web. Consequently, N isotope baselines of coastal waters may have changed over the past decades, especially where land use practices have shifted to intensified agriculture and where catchments have carried the excess N into coastal marine systems.

We used museum samples to reconstruct the isotopic compositions of 3 coastal fish species across 7 decades (1950–present). These 3 exclusively marine species occupy different TPs, habitats, and have distinct dietary niches. In order to separate isotopic shifts caused by (1) anthropogenic inputs or (2) natural environmental and ecological changes, we focused on a primary consumer 'baseline fish', the butterfish *Odax pullus*. *O. pullus* is an herbivorous fish from the Odacidae family found in kelp forests, usually shallower than 20 m (Roberts et al. 2015). It feeds mainly on kelp of the genera *Durvillaea*, *Macrocystis*, *Ecklonia*, *Lessonia*, and *Carpophyllum* (Russell 1983, Trip et al. 2014) and thus provides a valuable reference for resolving shifts in $\delta^{13}C$ and $\delta^{15}N$ baselines in primary producers. In contrast, tarakihi *Nemadactylus macro-*

pterus (Cheilodactylidae) and blue cod *Parapercis colias* (Pinguipedidae) have broad-spectrum diets, which allow them to adjust to changes in the composition and abundance of the prey field (Wing et al. 2012). While both are omnivores, *P. colias* can exploit higher trophic level prey such as fish, and *N. macropterus* feeds on a broad range of benthic and pelagic invertebrates including gastropods, bivalves, isopods, amphipods, polychaetes, crabs, echinoderms, and cephalochordates (Graham 1939, Russell 1983); this is reflected in its relatively lower TP. *O. pullus, N. macropterus*, and *P. colias* are common fish species that inhabit the Otago coast. Their importance is reflected in the recent creation of conservation plans (Nash 2018) and petitions (www.legasea.co.nz/TARAKIHI) with the goals of maintaining and enhancing stocks and understanding their feeding ecology.

We used isotope baseline proxies to follow the fishes' $\delta^{13}C$ and $\delta^{15}N$ baselines between the 1950s and 2018 and calculate $\delta^{15}N_{AA}$-based TP estimations to understand whether observed shifts were caused by a baseline shift or a change in the fishes' trophic ecology. We hypothesized that (1) the Suess effect will shift $\delta^{13}C$ values of all species of fish, and that it is possible to disentangle this effect on the $\delta^{13}C$ baseline from natural changes in the food web using analysis of $\delta^{13}C_{EAA}$; (2) the anthropogenic N inputs into coastal marine habitats will mostly affect the $\delta^{15}N$ baseline of *O. pullus* as a direct feeder of kelp, but less so the other 2 fish species with their omnivorous diets and wider niche.

2. MATERIALS AND METHODS

2.1. Experimental design and sample collection

All specimens of *Odax pullus*, *Nemadactylus macropterus*, and *Parapercis colias* used in the present study were collected from the Otago coast, a 480 km coastline on the south east of New Zealand's South Island. Past specimens, caught between the 1950s and 1990s, were acquired from Te Papa — National Museum of New Zealand (Wellington) and Otago Museum (Dunedin) collections (Table S1 in Supplement 1 at www.int-res.com/articles/suppl/m647p149_supp1.xlsx) and represent all available museum specimens from the Otago region. 'Present' samples, caught between 2017 and 2018, were provided by local anglers. In total, we collected 5 'past' and 5 'present' samples of *O. pullus*, 14 and 5 samples, respectively of *N. macropterus* and 6 and 11 samples, respectively, of *P. colias*. The size of a specimen is known to affect the isotopic values of muscle tissue (Dalponti et al. 2018, Ladds et al. 2020), and museum collections tend to be biased towards small specimens due to sampling and space limitations. In the present study, the distribution of the specimens' total length between past and present samples did not vary for *O. pullus* (279.8 ± 27.7 and 362 ± 27.7 mm) and *P. colias* (271.9 ± 35.4 and 344.9 ± 26.1) at a $p < 0.05$ level (Wilcoxon's non-parametric test). On the other hand, specimens of *N. macropterus* were significantly larger in the present (354.9 ± 16) than in past samples (208.2 ± 9.6). Muscle tissues (1 cm^3) from the dorsal musculature were collected from each fish for analysis. Prior to further preparation, muscle tissues sampled from museum collections were left in deionized water for 1 wk to allow excess preservatives to be washed out of the samples (Durante et al. 2020b). Fish muscle tissues were then oven-dried (60°C for 72 h) and subsequently ground with a mortar and pestle until yielding a fine and homogenous powder.

2.2. Bulk stable isotope analysis

A mass of 0.8–1.2 mg of dried fish muscle tissue was packed in tin capsules. All samples were analyzed in triplicate on a Europa 20-20 update stable isotope mass spectrometer (Europa Scientific) interfaced to a Carlo Erba elemental analyzer (NA1500; Carlo Erba) in continuous flow mode (precision: 0.2‰ for $\delta^{13}C$, 0.3‰ for $\delta^{15}N$) at the Iso-trace Research Lab in the Department of Chemistry, University of Otago. Results were calibrated using USG40 and USG41 reference materials (−26.24 and 37.76‰, respectively for C and −4.52 and 47.57‰, respectively for N) and EDTA standard (Elemental Microanalysis). Values were calculated and reported with respect to atmospheric N_2 (for $\delta^{15}N$ values) and Vienna Pee Dee Belemnite (VPDB) (for $\delta^{13}C$ values) international reference standards and reported in the standard delta notation (Fry 2006). Replicate samples were added between each 10 samples and among trays, to check for machine precision and accuracy.

Isotope results from preserved specimens were corrected for the effects of fixation, preservation, and differences in lipid content (for $\delta^{13}C$) using the equations from Durante et al. (2020b). These equations can be used for specimens fixed in formalin and preserved in ethanol or isopropanol for long periods of time and take into account the lipid content (parametrized by the C:N ratio) and proportion of N in the fish muscle tissue:

$$\delta^{15}N = 11.25 + 0.71 \times \delta^{15}N_{preserved} + 0.27 \times \delta^{13}C_{preserved} - 0.21 \text{ proportion of } N_{preserved} \quad (1)$$

$$\delta^{13}C_{lipid\ free} = -8.42 + 0.07 \times \delta^{15}N_{preserved} + 0.76 \times \delta^{13}C_{preserved} + 0.97 \times \text{preserved C:N}_{preserved} \quad (2)$$

where $\delta^{15}N$ and $\delta^{13}C_{lipid\ free}$ represent corrected values using $\delta^{15}N$, $\delta^{13}C$, proportion of N, and the C:N ratio from preserved specimens.

2.3. AA stable isotope analyses

AA stable isotope analyses were carried out in the Iso-trace Lab at the University of Otago. AAs were extracted by hydrolyzing 2.5 g of each sample with 2 ml 6 M HCl at 110°C for 24 h in a N_2 atmosphere. An internal standard, norleucine (50 µl of 1 mg ml^{-1} solution), was added to monitor the wet chemistry and AA stable isotope values. Solutes were then dried under a gentle flow of N_2 at 60°C and subsequently converted into *N*-Acetylisopropyl (*N*AIP, Fig. S1 in Supplement 2 at www.int-res.com/articles/suppl/m647p149_supp2.pdf) ester derivatives following the protocol described in (Sabadel et al. 2016), modified from (Styring et al. 2012). Details of the derivatization procedure can be found in Text S1 in Supplement 2. The $\delta^{13}C_{AA}$ and $\delta^{15}N_{AA}$ values were measured by a gas chromatography/combustion/isotope ratio mass spectrometer (GC-IRMS), using a Thermo Trace gas chromatograph, a GC combustion III interface, and a Delta^{plus} XP isotope ratio mass spectrometer (Thermo Fisher Scientific) (Text S2 in Supplement 2). Aliquots (200 nl) of derivatized AAs were injected, inlet at 270°C in splitless mode, carried by helium at 1.4 ml min^{-1} and separated on a VF-35ms column (0.32 mm i.d. and a 1.0 µm film thickness). The GC program can be found in Table S2 in Supplement 2. For $\delta^{13}C_{AA}$ measurements, the oxidation reactor was set at 950°C and the reduction reactor was left at room temperature; for $\delta^{15}N_{AA}$ measurements, the oxidation rector was set at 980°C, the reduction reactor at 650°C, and a liquid N_2 cold trap employed after the reduction reactor. Samples were analyzed in duplicates or triplicates (depending on sample reproducibility) along with AA standards of known isotopic composition (measured by elemental analyzer-IRMS). A total of 11 AAs from each sample were measured with no peak co-elutions, listed below. In order of elution: alanine (Ala), glycine (Gly), valine (Val), leucine (Leu), isoleucine (Ile), Threonine (Thr), serine (Ser), proline (Pro), aspargine + aspartic acid (Asx), glutamate + glutamic acid (Glx) and phenylalanine (Phe) (see Fig. S2 in Supplement 2 for a typical chromatogram). Note that during the hydrolysis step, asparagine is converted to aspartic acid (hence the notation Asx) and glutamate is converted to glutamic acid (hence the notation Glx). Raw $\delta^{13}C_{AA}$ was individually corrected relative to the AA $\delta^{13}C_{AA}$ of the standards to account for the added C and kinetic fractionation introduced during the derivatization procedure (Text S3 in Supplement 2). The δ values were reported following the conventional method of expressing δ at natural abundance, in per mil (‰), relative to an international standard: VPDB for $\delta^{13}C_{AA}$ and atmospheric N_2 for $\delta^{15}N_{AA}$ (Fig. S3 in Supplement 2). Precision (±1 SD) of corrected $\delta^{13}C_{AA}$ ranged from 0–1.7‰ with a mean of 0.4‰, while the precision for $\delta^{15}N_{AA}$ ranged from 0–1.7‰ with a mean of 0.4‰.

2.4. Trophic level estimations

TP based on AA isotope values were calculated using the $\delta^{15}N_{Glx}$ and $\delta^{15}N_{Phe}$ relationship ($TP_{Glx-Phe}$, Eq. 3) described in Chikaraishi et al. (2009):

$$TP_{Glx-Phe} = \frac{\left(\delta^{15}N_{Glx} - \delta^{15}N_{Phe} + \beta\right)}{TDF_{Glx-Phe}} + 1 \quad (3)$$

where β is the isotopic difference between Glx and Phe in the primary producers: $\delta^{15}N_{Glx} - \delta^{15}N_{Phe}$ = 3.4‰ for aquatic cyanobacteria and algae (Chikaraishi et al. 2009). The trophic discrimination factor, representing the difference in fractionation per TP of $\delta^{15}N_{Glx}$ and $\delta^{15}N_{Phe}$ ($TDF_{Glx-Phe}$), was chosen according to the fish species' diet (McMahon et al. 2015b). In their feeding experiment study, McMahon et al. (2015b) found that fishes fed on high protein diets, where the AA composition was similar to the fishes' muscle tissue, presented a smaller $TDF_{Glx-Phe}$ than fishes feeding on an herbivorous diet. Consequently, in the present study a $TDF_{Glx-Phe}$ value of 10.4‰ was used for the calculation of $TP_{Glx-Phe}$ of herbivores and of 7.2‰ for omnivores, respectively, matching the plant-based and omnivore diet from McMahon et al. (2015b). Uncertainties associated with the TP calculation using Eq. (3) were calculated by the propagation of errors following Dale et al. (2011) (Text S4 in Supplement 2).

2.5. Data treatment and statistical framework

For $\delta^{13}C_{EAA}$, data interpretation represented the $\delta^{13}C$ values of the following EAAs: Leu, Ile, Phe, Thr, and Val. For $\delta^{15}N_{AA}$ data interpretation, we only looked at a trophic AA (Glx) and a source AA (Phe).

To investigate trends of isotope values along the years, linear models were fitted to the data, and the slopes of the regression equations were compared between species and studies on the Suess effect. Linear models were run using JMP v.14 (SAS institute). Although our sample size was small and had a clustering nature, it met all the assumptions required to run linear regressions: normality (Q–Q plot of residuals), independence (residual by row number plot), and constant variance (residual plot) for most variables, except for $\delta^{13}C_{EAA}$ and $\delta^{15}N_{Phe}$ of *N. macropterus*. This suggested that a linear model did not fit this specific data very well, again due to the small sample size, and therefore some care had to be taken to avoid a biased result in any predictions or inferences made. Pairwise permutational ANOVA (PERMANOVA) tests were applied to the data to investigate differences in isotope values and TP estimates for each species before the peak of regional fertilizer use (1990) and present (2017 and 2018). PERMANOVA is an ANOVA that uses permutation to compute statistical tests instead of statistical tables, and does not assume linearity or normality (Anderson et al. 2008). Euclidian distances between samples of each species were used to compute resemblance matrices used in the PERMANOVA tests, which was run with unrestricted permutation of the raw data. PERMANOVAs were run on PRIMER v.6.1.2 (Clarke & Gorley 2006).

3. RESULTS

3.1. Bulk and AA C stable isotopes

The $\delta^{13}C_{Bulk}$ values of *Odax pullus* have significantly increased over time, from an average of −17.78‰ for past specimens to an average of −16.03‰ for muscle tissue samples collected in 2017–2018 (Table 1, Fig. 1), with an associated positive slope of 0.030 ± 0.011‰ (Table 2). On the other hand, $\delta^{13}C_{Bulk}$ values of our 2 omnivorous species have decreased over

Table 1. Mean (±SE) stable isotope values of carbon (bulk [$\delta^{13}C_{Bulk}$] and essential amino acids [$\delta^{13}C_{EAA}$]) and nitrogen ($\delta^{15}N_{Bulk}$, phenylalanine [$\delta^{15}N_{Phe}$]), and glutamic acid–amino acid-based estimated trophic position ($TP_{Glx-Phe}$), as well as the proportion of the omnivorous fish's diet supported by macroalgae (Macro%) from samples of historical and present material. Macro% was calculated based on $\delta^{15}N$ and $\delta^{13}C$ endmember values of macroalgae (8.42 and −15.50‰, respectively) and particulate organic matter (3.23 and −24.25‰, respectively) (L. M. Durante et al. unpubl. data). *t*-statistics from pairwise PERMANOVA tests are shown with their respective significance values (*p < 0.05; **p < 0.005; ***p < 0.0005)

Analysis	Species	Historical	Present	*t*
$\delta^{13}C_{Bulk}$	*Odax pullus*	−17.78 ± 0.34	−16.03 ± 0.45	3.084*
	Nemadactylus macropterus	−17.96 ± 0.24	−19.20 ± 0.19	2.924**
	Parapercis colias	−18.43 ± 0.22	−19.27 ± 0.35	1.671
$\delta^{13}C_{EAA}$	*O. pullus*	−19.79 ± 0.48	−20.41 ± 0.34	0.989
	N. macropterus	−19.46 ± 0.25	−22.79 ± 0.37	7.633***
	P. colias	−21.70 ± 0.17	−21.71 ± 0.55	4.38E−03
$\delta^{15}N_{Bulk}$	*O. pullus*	13.17 ± 0.44	12.24 ± 0.19	1.955
	N. macropterus	14.19 ± 0.23	13.39 ± 0.41	1.782
	P. colias	14.22 ± 0.19	14.01 ± 0.19	0.717
$\delta^{15}N_{Phe}$	*O. pullus*	10.47 ± 0.33	9.25 ± 0.37	2.492*
	N. macropterus	8.31 ± 0.48	5.69 ± 0.50	3.39**
	P. colias	7.31 ± 0.41	6.57 ± 0.85	0.735
$TP_{Glx-Phe}$	*O. pullus*	1.75 ± 0.07	1.70 ± 0.12	0.375
	N. macropterus	3.24 ± 0.05	3.67 ± 0.03	5.741***
	P. colias	3.67 ± 0.12	3.63 ± 0.09	0.274
Macro%	*N. macropterus*	0.56 ± 0.03	0.41 ± 0.03	2.946*
	P. colias	0.50 ± 0.03	0.40 ± 0.04	1.691

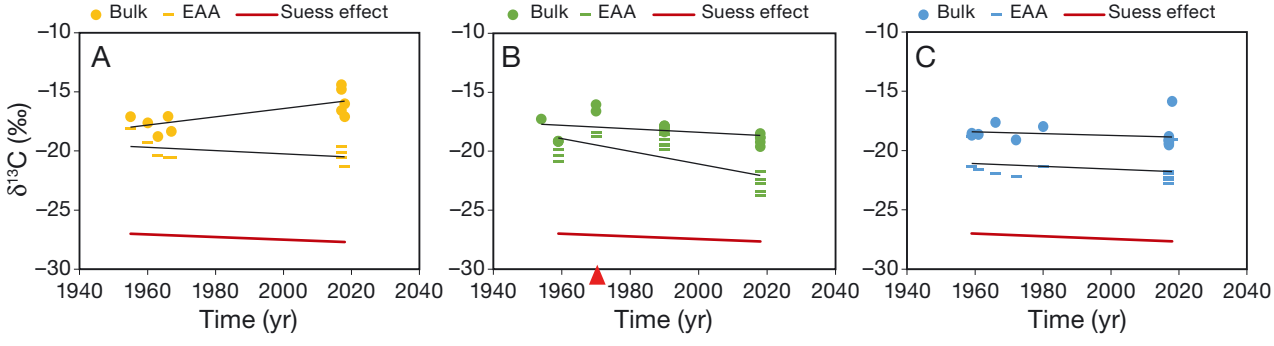

Fig. 1. Bulk and essential amino acid (EAA) $\delta^{13}C$ values for 3 coastal fish: (A) *Odax pullus*, (B) *Nemadactylus macropterus*, and (C) *Parapercis colias*. Triangle on the *x*-axis in (B) indicates the year of overfishing

Table 2. Linear regressions of C stable isotopes values for bulk ($\delta^{13}C_{Bulk}$) and averaged essential amino acids ($\delta^{13}C_{EAA}$), as well as $\delta^{15}N$ bulk values ($\delta^{15}N_{Bulk}$) and phenylalanine ($\delta^{15}N_{Phe}$) along with values for the predicted Suess effect in the ventilated South Pacific Ocean according to Eide et al. (2017). *p < 0.05; **p < 0.005

Factor	Species	r^2	Intercept ± SE	Slope ± SE	p
$\delta^{13}C_{Bulk}$	*Odax pullus*	0.5	−77.09 ± 21.12	0.030 ± 0.011	0.022*
	Nemadactylus macropterus	0.18	18.20 ± 19.20	−0.018 ± 0.010	0.074
	Parapercis colias	0.13	10.95 ± 19.58	−0.015 ± 0.010	0.147
$\delta^{13}C_{EAA}$	*O. pullus*	0.2	7.81 ± 21.2	−0.014 ± 0.010	0.23
	N. macropterus	0.49	86.71 ± 30.42	−0.054 ± 0.015	0.004**
	P. colias	2.2E−05	−22.06 ± 24.74	0.0002 ± 0.012	0.989
$\delta^{15}N_{Bulk}$	*O. pullus*	0.31	45.67 ± 17.28	−0.017 ± 0.009	0.093
	N. macropterus	0.22	52.11 ± 17.62	−0.019 ± 0.009	0.045*
	P. colias	0.05	24.39 ± 11.29	−0.005 ± 0.006	0.375
$\delta^{15}N_{Phe}$	*O. pullus*	0.48	55.94 ± 16.9	−0.023 ± 0.009	0.026*
	N. macropterus	0.33	99.60 ± 36.04	−0.046 ± 0.018	0.024*
	P. colias	0.4	29.72 ± 37.48	−0.011 ± 0.019	0.558
Suess effect		–	–	0.011 ± 0.001	–

time, from an average of −17.96‰ to an average of −19.20‰ for *Nemadactylus macropterus* ($p < 0.005$) and for *Parapercis colias*, from an average of −18.43‰ to an average of −19.27‰, although these differences were not significant in the later (Table 1, Fig. 1). Additionally, the slope of the linear regressions calculated for *N. macropterus* and *P. colias*, −0.018 ± 0.010 and −0.015 ± 0.010‰, respectively (Table 2), indicated that their change in $\delta^{13}C_{Bulk}$ values over time followed the Suess effect trend calculated for the ventilated South Pacific Ocean, which predicts a decrease of on average 0.011‰ yr^{-1} (−0.014 ± 0.001 [SD] to −0.006 ± 0.001‰) in $\delta^{13}C_{Bulk}$ (Eide et al. 2017).

To disentangle the factors likely responsible for the observed changes in $\delta^{13}C_{Bulk}$ values, we analyzed individual AA isotope values. As they are only synthesized in primary producers, EAAs can solely be acquired by higher trophic level species (TP = 2 and above) via their diets. Thus, $\delta^{13}C_{EAA}$ has often been used to track $\delta^{13}C$ baseline changes (Whiteman et al. 2019). In our data set, $\delta^{13}C_{EAA}$ were depleted relative to $\delta^{13}C_{Bulk}$ values, with differences ranging from 0.7–3.5‰ across the 3 species (Tables 1 & S3, the latter in Supplement 1; Fig. 1). For *O. pullus*, $\delta^{13}C_{EAA}$ values decreased over the past 7 decades from −19.79 to −20.41‰; and although the linear regression model between $\delta^{13}C_{EAA}$ and time was not significant, the value of the slope was found to be within that of the predicted Suess effect for the South Pacific region (−0.014 ± 0.010‰; Table 2). Similarly, *N. macropterus* presented a significant change in $\delta^{13}C_{EAA}$ values (from −19.46 to −22.79‰) and a much steeper and significant slope than the predicted bulk Suess effect (−0.054 ± 0.015‰). For both *O. pullus* and *N. macropterus*, the general trend was negative and in line with the decrease of environmental ^{13}C. However, for *P. colias* there were no significant changes in the $\delta^{13}C_{EAA}$ values (from −21.70 to −21.71‰), and the linear regression slope was flat (0.0002 ± 0.012‰; Table 2).

3.2. Bulk and AA N stable isotopes

$\delta^{15}N_{Bulk}$ values decreased over time for all 3 fish species studied as per their averaged values and calculated linear regression slopes, with differences that were significant for *N. macropterus*, but not for *O. pullus* and *P. colias* (Tables 1 & 2, Fig. 2). Additionally, significant temporal variation in the AA baseline $\delta^{15}N_{Phe}$ was observed for both *O. pullus* and *N. macropterus* (Fig. 3), where the N isotope baseline values dropped from an average of 10.47–9.25‰ and from 8.31–5.69‰, respectively (Table 1, Fig. 1); and although they decreased from an average of 7.31–6.57‰, variations of $\delta^{15}N_{Phe}$ in *P. colias* were not significant. Calculated coefficients from the linear regressions gave a slope of −0.023 ± 0.009‰ for *O. pullus*, meaning a change in the $\delta^{15}N_{phe}$ of *O. pullus* with time at a rate of 0.023‰ yr^{-1}. Similarly, linear regressions on $\delta^{15}N_{Phe}$ values with time showed a significant temporal trend for *N. macropterus* (−0.046 ± 0.018‰) and a non-significant but still negative trend in *P. colias* (−0.011 ± 0.019‰). Finally, *N. macropterus* had a distinct peak in $\delta^{15}N_{Bulk}$ as well as $\delta^{15}N_{Phe}$ values between 1970 and 1990 (Table S4 in Supplement 1, Fig. 3), followed by a significant decrease in present samples (Wilcoxon $Z = -1.84$, $p = 0.066$ for $\delta^{15}N$ and $Z = -2.76$, $p = 0.006$ for $\delta^{15}N_{Phe}$).

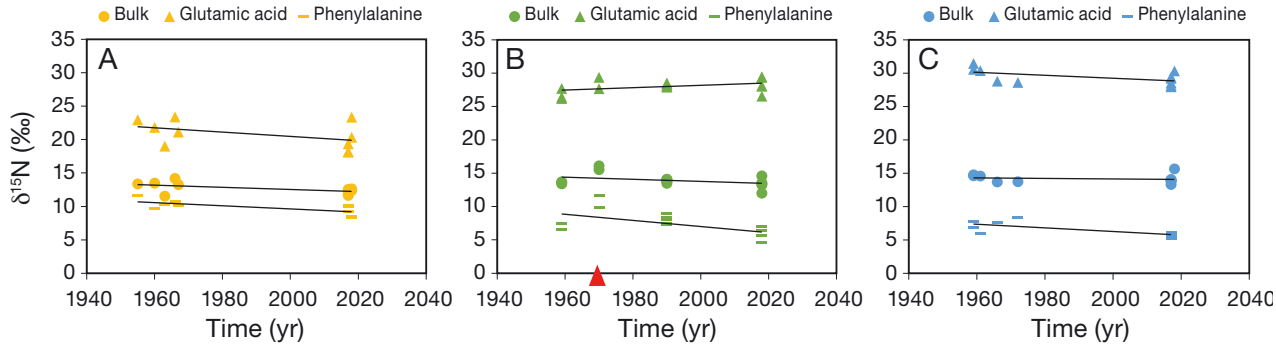

Fig. 2. Corrected $\delta^{15}N$ bulk , glutamic acid, and phenylalanine values for (A) *Odax pullus*, (B) *Nemadactylus macropterus*, and (C) *Parapercis colias*. Triangle on the *x*-axis in (B) indicates the year of overfishing

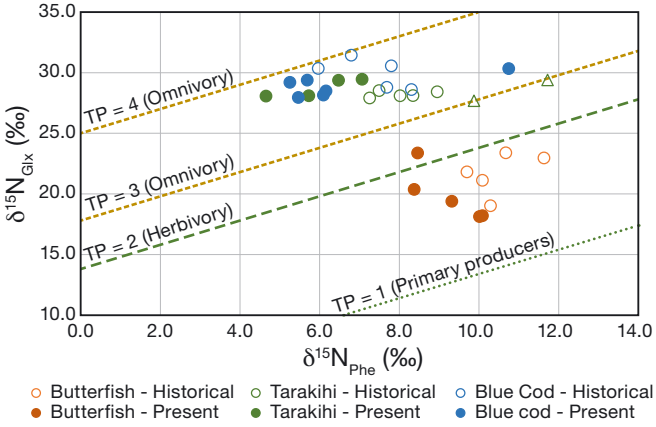

Fig. 3. Historical and present $\delta^{15}N$ values of the 2 canonical trophic and source amino acids: glutamic acid (Glx) and phenylalanine (Phe), respectively, from 3 coastal fish: *Odax pullus* (orange), *Nemadactylus macropterus* (green) and *Parapercis colias* (blue). Empty green triangles: samples of *N. macropterus* during a year of recorded high landings. Trophic position (TP) isoclines with a slope of 1.0 and *y*-intercept intervals corresponding to the appropriate trophic discrimination factor representing the difference in fractionation per TP of $\delta^{15}N_{Glx}$ and $\delta^{15}N_{Phe}$ of 10.4‰ for herbivores and 7.2‰ for omnivores following McMahon et al. (2015b), represent different TPs for fish species according to the equation by Chikaraishi et al. (2009)

3.3. Trophic structure estimates

Results from $TP_{Glx-Phe}$ of all samples were plotted as $\delta^{15}N_{Glx}$ against $\delta^{15}N_{phe}$ in Fig. 3, along with the trophic isoclines representing the different TPs calculated for herbivorous and omnivorous species according to their specific $TDF_{Glx-Phe}$ as discussed above. *O. pullus* data, past and present, were scattered around the herbivory trophic isocline (TP = 2), while past and present samples of *N. macropterus* and *P. colias* fitted as omnivorous, in between TP = 3 and 4. Average values of calculated $TP_{Glx-Phe}$ are displayed in Table 1. $TP_{Glx-Phe}$ indicated that both *O. pullus* and *P. colias* had no significant differences in their $TP_{Glx-Phe}$, from 1.75–1.70 and from 3.67–3.63, respectively. The reverse was observed for *N. macropterus*, where $TP_{Glx-Phe}$ had a significant increase between past and present periods, from 3.24–3.67 (Table 1).

4. DISCUSSION

4.1. Suess effect in reef fish as reflected in C stable isotopes

Because *Odax pullus* is a primary consumer with a narrow diet niche mainly consisting of macroalgae, its isotope chemistry represents an interesting proxy for tracking the isotopic baseline changes in organic matter source through time. However, in our study $\delta^{13}C_{Bulk}$ and $\delta^{13}C_{EAA}$ values of *O. pullus* samples indicated contrasting trends, with $\delta^{13}C_{Bulk}$ values going against the Suess effect. This interesting contradiction challenges the chemical preservation correction equations that were used in our study, but more broadly, the general use of bulk isotopes from preserved samples. Here, we can anticipate some variation in accuracy using the correction Eqs. (1) and (2) on samples of *O. pullus*, as (1) chemical preservation effects are dependent on lipid concentrations and compositions, and thus the C:N ratio of the samples (Kelly et al. 2006); (2) herbivorous fish have higher C:N ratio than omnivorous or carnivorous fishes (Mill et al. 2007); and (3) the equation from Durante et al. (2020b) was not developed using herbivorous fishes. Consequently, it is likely that the increase in $\delta^{13}C_{Bulk}$ values observed for *O. pullus* were directly linked to the non-adapted corrections made to the values. Therefore, narrowing on the isotopic values of specific compounds that are not affected by chemical preservation can help resolve shifts in C baselines more precisely. Focusing on $\delta^{13}C_{EAA}$ values of our herbivorous fish,

the slope of the regression equation indicates that macroalgae has undergone a change in isotopic composition with the same direction and amplitude estimated for the Suess effect on $\delta^{13}C_{Bulk}$ values for the Southern Pacific Ocean (Eide et al. 2017). The Suess effect on $\delta^{13}C_{EAA}$ in the Otago coastal environment, as observed in samples of *O. pullus*, decreased on average by 0.014‰ yr^{-1} between 1950 and 2018.

While both omnivorous species' $\delta^{13}C_{Bulk}$ values followed the predicted Suess effect, it was not as clearly reflected in their $\delta^{13}C_{EAA}$ values. Indeed, the Suess effect is likely to be masked by the complexity of the fishes' movements and diets. For *P. colias*, no significant shifts in the C isotopic baseline were found, suggesting no significant change at the base of the food web supporting this species. *N. macropterus* underwent large shifts in $\delta^{13}C_{EAA}$ through time, indicating a likely change in both food web baseline and species resource use. The $\delta^{13}C_{EAA}$ values were much lower than $\delta^{13}C_{Bulk}$, indicating that the $\delta^{13}C_{Bulk}$ values were influenced by other molecules contained in the fish tissues, such as non-essential AAs which can be synthesized de novo by the fish and therefore are not representative of the C isotopic baseline.

4.2. Anthropogenic influence of the N isotopic baseline or regional N enrichment effect

The N isotopic baseline values of *O. pullus*, both $\delta^{15}N_{Bulk}$ and $\delta^{15}N_{Phe}$, also decreased over time. However, the difference in significance of the linear regressions between $\delta^{15}N_{Bulk}$ and $\delta^{15}N_{Phe}$ values suggested that by looking at the molecular level, i.e. using Phe as an isotopic baseline, we can acquire more precise results that are not affected by other metabolic processes and biases when compared to bulk analysis. Moreover, $\delta^{15}N_{Phe}$ has been previously shown to not be affected by the fish's diet (herbivorous vs. omnivorous/carnivorous) (McMahon et al. 2015b). Additionally, calculated coefficients from the linear regressions indicated that the $\delta^{15}N_{phe}$ of *O. pullus* changed at a rate of 0.023‰ yr^{-1} between 1950 and 2018. Given that *O. pullus* is known to be exclusively herbivorous, mainly feeding on kelp, and that its calculated $TP_{Glx-Phe}$ has remained unchanged over the last 7 decades (~1.70–1.75), the observed shifts in its $\delta^{15}N_{phe}$ over time indicate that the $\delta^{15}N$ at the base of the local food web has changed. A shift in $\delta^{15}N_{phe}$ can be linked to a wide range of phenomena occurring in the local environment and mechanisms for lowering baseline $\delta^{15}N$ values. For example, an increasing rate of N_2-fixation; relative decrease in denitrification rates; increases in nutrient availability leading to greater expression of isotopic fractionation by primary producers; changes in N biogeochemical cycling (e.g. availability of ammonium vs. nitrate) or atmospheric N deposition (Montoya et al. 2002, Mompeán et al. 2013, 2016, Loick-Wilde et al. 2019). However, in our local ecosystem, the change in the N isotopic baseline was likely related to increases in nutrient inputs from anthropogenic sources including synthetic fertilizers, and increases in turbidity from inputting particulate organic N along the Otago coast over the past decades (Vander Zanden et al. 2005, Parfitt et al. 2012, Schallenberg et al. 2017). Indeed, the expanded use of agricultural inorganic fertilizer in New Zealand led to an increase of N inputs in the Otago region by 450% between 1990 and 2001, reaching 530% by 2010 (Parfitt et al. 2012). Further, a study by Heggie & Savage (2009) in the Otago region modeled the different N contributions into coastal water and found a significant contribution of fertilizers used by nearby agricultural land. Inorganic fertilizers are depleted in $\delta^{15}N$ (Heaton 1986, Valiela et al. 2000) and they leach into the oceans and are incorporated into marine food webs through primary consumers (Vander Zanden et al. 2005), creating a regional N enrichment effect.

While both species that were sampled from the Otago coast were omnivorous, the effect of local inorganic N inputs on *N. macropterus* and *P. colias* baseline $\delta^{15}N$ values was different through time. On one hand, nothing seems to have significantly affected the $\delta^{15}N$ (bulk and AA) isotopic composition of *P. colias*. However, decreased values of $\delta^{13}C_{Bulk}$ from this species' muscle tissue indicate a smaller reliance on macroalgal productivity to its food web compared to *O. pullus*. *P. colias* is a large coastal demersal fish species with a broad omnivorous diet and a limited home range (Russell 1983, Carbines & Beentjes 2003, Rodgers & Wing 2008, Roberts et al. 2015). Its broad diet allows this species to adapt to different prey fields and organic matter baselines, filling the role of a multichannel omnivore in coastal reef communities (Wing et al. 2012). However adaptive, its $TP_{Glx-Phe}$ remained constant through time, with a TP of ~3.6 (omnivore). On the other hand, *N. macropterus* has shown dramatic changes in both bulk and AA isotope signatures over time, with contrasting trends when compared to the other 2 species. Furthermore, a general linear model based on a large data set (encompassing the present data set) showed that length has a significant negative effect on $\delta^{15}N_{Bulk}$, whether including or excluding museum specimens (L. M.

Durante et al. unpubl. data). This is likely caused by the life movements of *N. macropterus*. *N. macropterus* is a demersal fish that inhabits waters from surface to almost 500 m depth (McKenzie et al. 2017), feeding on a broad range of infaunal and epifaunal invertebrates by ingestion of sediment (Godfriaux 1974). As it gets older, *N. macropterus* tends to forage in deeper water, moving along a $\delta^{15}N_{Bulk}$ decreasing gradient. Because of its dietary niche, i.e. dependency on infaunal invertebrate prey, *N. macropterus* is highly susceptible to habitat degradation from trawling activities and overfishing. In fact, isotope values and TP results are consistent with the effects of increased fishing pressure as indicated by fish landing data for this species (Fisheries New Zealand 2019, Durante et al. 2020a). During a period of large fisheries landings in the 1970s, the $\delta^{13}C$ and $\delta^{15}N$ values of *N. macropterus* increased, while its TP decreased. The observed pattern is consistent with a change in habitat, with higher $\delta^{13}C$ and $\delta^{15}N$ values indicating a larger reliance on macroalgae basal production with a drop in the TP towards TP ~ 3. Following the observed peak in reliance on organic matter derived from macroalgae, there was a significant decrease in $\delta^{15}N_{Phe}$ values and an increase in $TP_{Glx–Phe}$, which indicates a shift towards relying on a more pelagic-based food web, with increased TP along with its $\delta^{13}C$ and $\delta^{15}N$ values. Therefore, changes in isotope values of *N. macropterus* were likely to have been influenced by other factors, such as the direct (e.g. specimen removal) and indirect (e.g. habitat degradation) effects of fishing (Hinz et al. 2017). Although outside the scope of the present study, these considerations corroborate the most recent stock assessment for the species, which demonstrated that *N. macropterus* stocks were overfished inside the east coast of the South Island in recent years with a biomass significantly below the soft limit (Fisheries New Zealand 2019).

4.3. Caveats and future studies

In the present study, we found that (1) the Suess effect, a decrease in the value of the $\delta^{13}C$ isotopic baseline — whether bulk or AA — has impacted the $\delta^{13}C$ of the 3 species of fish considered in our study. Further, it was possible to disentangle this effect from natural changes in food web position using values of $\delta^{13}C_{AA}$. In addition, (2) the regional N-enrichment effect, a change in the value of N isotopic baseline, was highlighted and calculated to be 0.023‰ yr^{-1} for our specific coastal region over the last 7 decades, evident from analysis of the herbivorous species *O. pullus*. These findings highlight the necessity of considering temporal shifts in isotopic baselines in coastal systems affected by anthropogenic activities when undertaking studies of trophic ecology. Below are a few issues that require consideration in the context of resolving changes to C and N isotopic baselines.

First, because museums prefer to preserve smaller specimens for easy keeping, samples representing past time periods used in the present study are biased towards smaller individuals compared to present-day specimens. Although this could have influenced our TP estimates, since larger specimens tend to feed on larger prey and therefore occupy a higher TP, our results do not corroborate that idea. Moreover, studies have demonstrated that although body size is a good predictor of TP at a community level, there is no clear trend within species (Jennings et al. 2001), and those relationships are more related to ontogenetic shifts and size of niche breadth displayed by each species (Dalponti et al. 2018, Ladds et al. 2020). Nevertheless, including size in statistical models provides a test of this potential bias.

Second, Durante et al. (2020b) demonstrated that preservation followed by fixation has a significant effect of increasing $\delta^{15}N_{AA}$ values of fish muscle tissue. Although the shifts in $\delta^{15}N_{AA}$ followed the same trend among different AAs (which allows researchers to accurately calculate $TP_{Glx–Phe}$ using the relationship between $\delta^{15}N_{Glx}$ and $\delta^{15}N_{Phe}$), the analysis of a single AA could incur bias. In that work, Durante et al. (2020b) discussed the possibility that changes in $\delta^{15}N_{AA}$ were caused by bacterial attack due to poor sample storage prior to fixation. In their study, 2 species were analyzed for $\delta^{15}N_{AA}$: *P. colias* was collected on a research cruise and rapidly processed; *Seriolella brama* was acquired from local commercial fishers. The time between catching and processing *S. brama* in the lab could have caused the discrepancies between species reported in Durante et al. (2020b). Since the museum specimens in our study were usually collected close to shore by researchers, or during research cruises and processed immediately after collection, either frozen or fixed, we can assume those samples did not have time to undergo the bacterial attack that was previously reported to cause changes in $\delta^{15}N_{AA}$ (Durante et al. 2020b).

Finally, although the sample sizes of the present study can be considered small for each time period (n = 5–10), these samples comprise all the available museum specimens from the Otago region and therefore provide unique and novel insights about

biochemical cycles and food web structure in past environments that we no longer can sample. Although there was variation among samples, all species showed a clear general trend in isotopic shifts with time, which can help inform our understanding of legacy effects in marine coastal environments. These observations are key to determining how past environments have changed as a result of anthropogenic influences on food web structures and biogeochemical cycles of C and N in coastal marine ecosystems.

Acknowledgements. We thank Carl Struthers, Clive Roberts, Andrew Stewart (Te Papa – National Museum of New Zealand) and Kane Fleury (Otago Museum) for their expertise, contribution, and support of our work. Technical support was provided by Robert van Hale, Dianne Clark, Doug Mackie, Linda Groenewegen, and Reuben Pooley from the Departments of Marine Science and Chemistry at Otago University. Monetary support was provided from a National Science Challenge: Sustainable Seas (4.1.1 Ecosystem Connectivity) grant to S.R.W. L.M.D. was additionally supported by a University of Otago PhD scholarship, and A.J.M.S. was supported by the Sustainable Seas National Science Challenge (4.1.1 Ecosystem Connectivity).

LITERATURE CITED

Anderson M, Gorley RN, Clarke KR (2008) PERMANOVA+ for PRIMER: guide to software and statistical methods. PRIMER-E, Plymouth

Baker DM, Webster KL, Kim K (2010) Caribbean octocorals record changing carbon and nitrogen sources from 1862 to 2005. Glob Change Biol 16:2701–2710

Carbines GD, Beentjes MP (2003) Relative abundance of blue cod in Dusky Sound in 2002. New Zealand fisheries assessment report 2003/37. Ministry of Fisheries, Wellington

Chikaraishi Y, Ogawa NO, Kashiyama Y, Takano Y and others (2009) Determination of aquatic food-web structure based on compound-specific nitrogen isotopic composition of amino acids. Limnol Oceanogr Methods 7:740–750

Chua KWJ, Liew JH, Shin KH, Yeo DCJ (2020) Effects of ethanol preservation and formalin fixation on amino acid stable isotope analysis ($\delta^{13}C$ and $\delta^{15}N$) and its ecological applications. Limnol Oceanogr Methods 18:77–88

Clarke KR, Gorley RN (2006) PRIMER v6: user manual/tutorial. PRIMER-E, Plymouth

Dale JJ, Wallsgrove NJ, Popp BN, Holland KN (2011) Nursery habitat use and foraging ecology of the brown stingray *Dasyatis lata* determined from stomach contents, bulk and amino acid stable isotopes. Mar Ecol Prog Ser 433:221–236

Dalponti G, Guariento RD, Caliman A (2018) Hunting high or low: body size drives trophic position among and within marine predators. Mar Ecol Prog Ser 597:39–46

Durante LM, Beentjes MP, Wing SR (2020a) Shifting trophic architecture of marine fisheries in New Zealand: implications for guiding effective ecosystem-based management. Fish Fish 21:813–830

Durante LM, Sabadel AJM, Frew RD, Ingram T, Wing SR (2020b) Effects of fixatives on stable isotopes of fish muscle tissue: implications for trophic studies on preserved specimens. Ecol Appl 30:e02080

Eide M, Olsen A, Ninnemann US, Eldevik T (2017) A global estimate of the full oceanic ^{13}C Suess effect since the preindustrial. Global Biogeochem Cycles 31:492–514

Felix JD, Elliott EM (2013) The agricultural history of human–nitrogen interactions as recorded in ice core $\delta^{15}N\text{-}NO_3^-$. Geophys Res Lett 40:1642–1646

Fisheries New Zealand (2019) Stock assessments and stock status. Fisheries Assessment Plenary, Ministry for Primary Industries, Wellington

Fry B (2006) Stable isotope ecology. Springer-Verlag, New York, NY

Godfriaux BL (1974) Food of Tarakihi in western Bay of Plenty and Tasman Bay, New Zealand. N Z J Mar Freshw Res 8:111–153

Graham DH (1939) Food of the fishes of Otago Harbour and Adjacent Sea. Trans Proc R Soc NZ 68:421–436

Gruber N, Keeling CD, Bacastow RB, Guenther PR and others (1999) Spatiotemporal patterns of carbon-13 in the global surface oceans and the oceanic Suess effect. Global Biogeochem Cycles 13:307–335

Hannides CCS, Popp BN, Landry MR, Graham BS (2009) Quantification of zooplankton trophic position in the North Pacific Subtropical Gyre using stable nitrogen isotopes. Limnol Oceanogr 54:50–61

Harley CDG, Hughes AR, Hultgren KM, Miner BG and others (2006) The impacts of climate change in coastal marine systems. Ecol Lett 9:228–241

Heaton THE (1986) Isotopic studies of nitrogen pollution in the hydrosphere and atmosphere: a review. Chem Geol Isot Geosci Sect 59:87–102

Heggie K, Savage C (2009) Nitrogen yields from New Zealand coastal catchments to receiving estuaries. NZ J Mar Freshw Res 43:1039–1052

Hetherington ED, Olson RJ, Drazen JC, Lennert-Cody CE, Ballance LT, Kaufmann RS, Popp BN (2017) Spatial food-web structure in the eastern tropical Pacific Ocean based on compound-specific nitrogen isotope analysis of amino acids. Limnol Oceanogr 62:541–560

Hetherington ED, Kurle CM, Ohman MD, Popp BN (2019) Effects of chemical preservation on bulk and amino acid isotope ratios of zooplankton, fish, and squid tissues. Rapid Commun Mass Spectrom 33:935–945

Hinz H, Moranta J, Balestrini S, Sciberras M and others (2017) Stable isotopes reveal the effect of trawl fisheries on the diet of commercially exploited species. Sci Rep 7: 6334

Hundey EJ, Russell SD, Longstaffe FJ, Moser KA (2016) Agriculture causes nitrate fertilization of remote alpine lakes. Nat Commun 7:10571

Jennings S, Pinnegar JK, Polunin NVC, Boon TW (2001) Weak cross-species relationships between body size and trophic level belie powerful size-based trophic structuring in fish communities. J Anim Ecol 70:934–944

Keeling CD (1979) The Suess effect: ^{13}Carbon–^{14}Carbon interrelations. Environ Int 2:229–300

Kelly B, Dempson JB, Power M (2006) The effects of preservation on fish tissue stable isotope signatures. J Fish Biol 69:1595–1611

Ladds MA, Pinkerton MH, Jones E, Durante LM, Dunn MR (2020) Relationship between morphometrics and trophic levels in deep-sea fishes. Mar Ecol Prog Ser 637:225–235

Loick-Wilde N, Fernández-Urruzola I, Eglite E, Liskow I and others (2019) Stratification, nitrogen fixation, and cyanobacterial bloom stage regulate the planktonic food web structure. Glob Change Biol 25:794–810

Marion GS, Dunbar RB, Mucciarone DA, Kremer JN, Lansing JS, Arthawiguna A (2005) Coral skeletal $\delta^{15}N$ reveals isotopic traces of an agricultural revolution. Mar Pollut Bull 50:931–944

McKenzie JR, Beentjes M, Parker S, Parsons DM and others (2017) Fishery characterisation and age composition of tarakihi in TAR 1, 2 and 3 for 2013/14 and 2014/15. New Zealand Fisheries assessment report; 2017/36. Ministry for Primary Industries, Wellington. http://fs.fish.govt.nz/Doc/24477/FAR-2017-36-Tarakihi-age-composition.pdf.ashx

McMahon KW, McCarthy MD, Sherwood OA, Larsen T, Guilderson TP (2015a) Millennial-scale plankton regime shifts in the subtropical North Pacific Ocean. Science 350:1530–1533

McMahon KW, Thorrold SR, Elsdon TS, McCarthy MD (2015b) Trophic discrimination of nitrogen stable isotopes in amino acids varies with diet quality in a marine fish. Limnol Oceanogr 60:1076–1087

McMahon KW, Thorrold SR, Houghton LA, Berumen ML (2016) Tracing carbon flow through coral reef food webs using a compound-specific stable isotope approach. Oecologia 180:809–821

Mill AC, Pinnegar JK, Polunin NVC (2007) Explaining isotope trophic-step fractionation: why herbivorous fish are different. Funct Ecol 21:1137–1145

Mompeán C, Bode A, Benítez-Barrios VM, Domínguez-Yanes JF, Escánez J, Fraile-Nuez E (2013) Spatial patterns of plankton biomass and stable isotopes reflect the influence of the nitrogen-fixer *Trichodesmium* along the subtropical North Atlantic. J Plankton Res 35:513–525

Mompeán C, Bode A, Gier E, McCarthy MD (2016) Bulk vs. amino acid stable N isotope estimations of metabolic status and contributions of nitrogen fixation to size-fractionated zooplankton biomass in the subtropical N Atlantic. Deep Sea Res I 114:137–148

Montoya JP, Carpenter EJ, Capone DG (2002) Nitrogen fixation and nitrogen isotope abundances in zooplankton of the oligotrophic North Atlantic. Limnol Oceanogr 47: 1617–1628

Nash HS (2018) Blue cod national strategy. Fisheries New Zealand, Wellington

O'Connell TC (2017) 'Trophic' and 'source' amino acids in trophic estimation: a likely metabolic explanation. Oecologia 184:317–326

Parfitt RL, Stevenson BA, Dymond JR, Schipper LA, Baisden WT, Ballantine DJ (2012) Nitrogen inputs and outputs for New Zealand from 1990 to 2010 at national and regional scales. N Z J Agric Res 55:241–262

Pomerleau C, Heide-Jørgensen MP, Ferguson SH, Stern HL, Høyer JL, Stern GA (2017) Reconstructing variability in West Greenland ocean biogeochemistry and bowhead whale (*Balaena mysticetus*) food web structure using amino acid isotope ratios. Polar Biol 40: 2225–2238

Popp BN, Graham BS, Olson RJ, Hannides CCS and others (2007) Insight into the trophic ecology of yellowfin tuna, *Thunnus albacares*, from compound-specific nitrogen isotope analysis of proteinaceous amino acids. In: Dawson TE, Siegwolf RTW (eds) Stable isotopes as indicators of ecological change. Elsevier, Amsterdam, p 173–190

Roberts CD, Stewart AL, Struthers CD (2015) The fishes of New Zealand. Te Papa Press, Wellington

Rodgers KL, Wing SR (2008) Spatial structure and movement of blue cod *Parapercis colias* in Doubtful Sound, New Zealand, inferred from $\delta^{13}C$ and $\delta^{15}N$. Mar Ecol Prog Ser 359:239–248

Ruiz-Cooley RI, Koch PL, Fiedler PC, McCarthy MD (2014) Carbon and nitrogen isotopes from top predator amino acids reveal rapidly shifting ocean biochemistry in the outer California Current. PLOS ONE 9:e110355

Russell BC (1983) The food and feeding habits of rocky reef fish of north-eastern New Zealand. N Z J Mar Freshw Res 17:121–145

Sabadel AJM, Woodward EMS, Van Hale R, Frew RD (2016) Compound-specific isotope analysis of amino acids: a tool to unravel complex symbiotic trophic relationships. Food Webs 6:9–18

Sabadel AJM, Van Oostende N, Ward BB, Woodward EMS, Van Hale R, Frew RD (2019) Characterization of particulate organic matter cycling during a summer North Atlantic phytoplankton bloom using amino acid C and N stable isotopes. Mar Chem 214:103670

Schallenberg M, Hamilton DP, Hicks AS, Robertson HA and others (2017) Multiple lines of evidence determine robust nutrient load limits required to safeguard a threatened lake/lagoon system. N Z J Mar Freshw Res 51:78–95

Schiff JT, Batista FC, Sherwood OA, Guilderson TP and others (2014) Compound specific amino acid $\delta^{13}C$ patterns in a deep-sea proteinaceous coral: implications for reconstructing detailed $\delta^{13}C$ records of exported primary production. Mar Chem 166:82–91

Shackell NL, Frank KT, Fisher JAD, Petrie B, Leggett WC (2010) Decline in top predator body size and changing climate alter trophic structure in an oceanic ecosystem. Proc R Soc B 277:1353–1360

Styring AK, Kuhl A, Knowles TDJ, Fraser RA, Bogaard A, Evershed RP (2012) Practical considerations in the determination of compound-specific amino acid $\delta^{15}N$ values in animal and plant tissues by gas chromatography-combustion-isotope ratio mass spectrometry, following derivatisation to their N-acetylisopropyl esters. Rapid Commun Mass Spectrom 26:2328–2334

Thrush SF, Townsend M, Hewitt JE, Davies K, Lohrer AM, Lundquist C, Cartner K (2013) The many uses and values of estuarine ecosystems. In: Dymond J (ed) Ecosystem services in New Zealand: conditions and trends. Manaaki Whenua Press, Lincoln, p 226–237

Trip EDL, Clements KD, Raubenheimer D, Choat JH (2014) Temperature-related variation in growth rate, size, maturation and life span in a marine herbivorous fish over a latitudinal gradient. J Anim Ecol 83:866–875

Valiela I, Geist M, McClelland J, Tomasky G (2000) Nitrogen loading from watersheds to estuaries: verification of the Waquoit Bay nitrogen loading model. Biogeochemistry 49:277–293

Van Hale R, Frew RD (2010) Rayleigh distillation equations applied to isotopic evolution of organic nitrogen across a continental shelf. Mar Freshw Res 61:369–378

Vander Zanden MJ, Vadeboncoeur Y, Diebel MW, Jeppesen E (2005) Primary consumer stable nitrogen isotopes as indicators of nutrient source. Environ Sci Technol 39: 7509–7515

Vokhshoori NL, McCarthy MD, Collins PW, Etnier MA and others (2019) Broader foraging range of ancient short-tailed albatross populations into California coastal waters based on bulk tissue and amino acid isotope analysis. Mar Ecol Prog Ser 610:1–13

Whiteman JP, Elliott Smith EA, Besser AC, Newsome SD (2019) A guide to using compound-specific stable isotope analysis to study the fates of molecules in organisms and ecosystems. Diversity (Basel) 11:8

Wing SR, Beer NA, Jack L (2012) Resource base of blue cod *Parapercis colias* subpopulations in marginal fjordic habitats is linked to chemoautotrophic production. Mar Ecol Prog Ser 466:205–214

Yamaguchi YT, McCarthy MD (2018) Sources and transformation of dissolved and particulate organic nitrogen in the North Pacific Subtropical Gyre indicated by compound-specific $\delta^{15}N$ analysis of amino acids. Geochim Cosmochim Acta 220:329–347

Zupcic-Moore JR, Ruiz-Cooley RI, Paliza O, Koch PL, McCarthy MD (2017) Using stable isotopes to investigate foraging variation and habitat use of sperm whales from northern Peru. Mar Ecol Prog Ser 579:201–212

Editorial responsibility: James McClintock, Birmingham, Alabama, USA

Submitted: April 28, 2020; Accepted: July 2, 2020
Proofs received from author(s): August 9, 2020